IEEE Access
Multidisciplinary | Rapid Review | Open Access Journal

Received August 31, 2018, accepted November 13, 2018, date of publication November 23, 2018, date of current version December 27, 2018.

Digital Object Identifier 10.1109/ACCESS.2018.2883175

Thermal Analysis of Averaging Times in Radio-Frequency Exposure Limits Above 1 GHz

KENNETH R. FOSTER[1], (Life Fellow, IEEE), MARVIN C. ZISKIN[2], (Life Fellow, IEEE), QUIRINO BALZANO[3], (Life Fellow, IEEE), AND AKIMASA HIRATA[4], (Fellow IEEE)
[1]Department of Bioengineering, University of Pennsylvania, Philadelphia, PA 19104 USA
[2]Temple University School of Medicine, Philadelphia, PA 19140 USA
[3]Department of Electrical and Computer Engineering, University of Maryland at College Park, College Park, MD 20742 USA
[4]Department of Electrical and Mechanical Engineering, Nagoya Institute of Technology, Nagoya 466-8555, Japan

Corresponding author Kenneth R. Foster (kfoster@seas.upenn.edu)

The work of K. R. Foster, M. C. Ziskin, and Q. Balzano was supported in part by Mobile and Wireless Forum.

ABSTRACT This paper considers the problem of choosing an appropriate ''averaging time'' in radiofrequency (RF) exposure limits to protect against thermal hazards, focusing on the RF frequency range above 3–10 GHz. Analysis is based on examination of the dynamic properties of thermal models for tissue using Pennes' bioheat equation. Three models are considered: a baseline model consisting of a uniform half space with dielectric and thermal properties similar to those of human skin with adiabatic boundary conditions; a layered 1D model with dielectric and thermal properties similar to those of skin, fat, and underlying muscle, with convective boundary conditions appropriate for room environments; and exposures to the head of an anatomically detailed image-based model (''Taro''). RF exposure consisted of plane wave radiation incident on the two planar models, and radiation from resonant dipoles located 1.5 cm from the head model, at frequencies ranging from 1 to 300 GHz. The dynamic properties of the models were explored by analytic solution of the baseline model, and from numerical solutions of the thermal responses of the layered and head models. From the step responses of the models (increases in surface temperature to a suddenly imposed exposure), the impulse and frequency responses of the models were obtained. In the frequency domain, the thermal models exhibit extreme lowpass characteristics with cutoff (−3 dB response) frequencies below 1 mHz. The impulse response to millimeter wave radiation (30–300 GHz) shows a sharp peak at zero time, due to short term accumulation of heat near the surface, which dissipates quickly as heat is conducted into deeper layers of tissue. Simple analytical results of a further simplified model assuming purely surface heating agree well with results of a more detailed assessment for millimeter waves. Response of the model to pulse trains and to single maximum fluence ''big bang'' pulses in which all allowable energy over a 6-min averaging time is delivered in one short pulse raises the possibility of excessive transient temperature increases at the tissue surface from exposure to short high-fluence pulses at mm-wave frequencies. Such exposures are not produced by current technologies apart from certain military weapons systems but may occur from future high-power mm-wave technology. By contrast, simulations of exposure from a communications waveform at 1.9 GHz show extremely tiny transient temperature fluctuations. The results generally confirm the present choice of 6 min for an averaging time in the current generation of RF exposure limits but suggest the need for additional limits on fluence for brief high-fluence pulses at mm-wave frequencies. This paper addresses thermal hazards only, and a larger range of evidence would need to be evaluated as well in revising exposure limits.

INDEX TERMS Radiofrequency safety, exposure limits, bioheat equation.

I. INTRODUCTION

Widely accepted exposure guidelines for human exposure to radiofrequency (RF) energy (e.g. Federal Communications Commission (FCC) [1], IEEE C95.1-2005 [2] and ICNIRP 1998 [3]) specify ''averaging times'' over which exposure is to be averaged for purposes of compliance assessment (Table 1). The averaging times are 6 or 30 minutes over most RF frequencies, but they decrease in the IEEE

TABLE 1. Averaging times in exposure limits*.

Standard/ Guideline	General public/ lower tier, min	Occupational/upper tier, min
FCC (1997)	30 (mobile devices or far field exposure) 30 (portable devices)	6 (mobile devices or far field exposure) 6 (portable devices)
IEEE C95.1-2005 Maximum permissible exposure (MPE)	0.1-30 MHz 6	0.1 MHz-3 GHz 6
	30-100 MHz $0.0636\ f_M^{1.337}$	
	100 MHz – 5 GHz 30	
	5-30 GHz $150/f_G$	3-30 GHz $19.63/f_G^{1.079}$
	30-100 GHz $25.24/\ f_G^{0.476}$	30-300 GHz $2.524/f_G^{0.476}$
	100-300 GHz $5048/[(9\ f_G–700)f_G^{0.476}]$	
ICNIRP (1998) Basic restrictions and reference levels	6 (<10 GHz) $68/f_G^{1.05}$ (10-300 GHz)	6 (<10 GHz) $68/f_G^{1.05}$ (10-300 GHz)

(f_M frequency in MHz, f_G frequency in GHz; all times in min)

and ICNIRP limits with frequency above 3-10 GHz to reach 10 seconds at the upper end of the frequency range covered by the limits (300 GHz) where the limits meet up with exposure limits for infrared energy.

Choosing an appropriate averaging time is important in the design of exposure limits to protect against thermal hazards. Excessively long averaging times will permit excessive short-term exposures, while too-short times will be overly conservative by excluding short term fluctuations in exposure that are thermally innocuous.

Averaging times in present limits have generally been set on the basis of *ad hoc* approximations and back-of-the-envelope calculations. According to Thomas S. Ely (1924-2015), who participated in the development of the first RF exposure limit in the U.S. during the 1960s (USAS C95.1; 1966), the committee recognized the need to average exposure over time to account for the thermal inertia of tissue. Ely wrote [4] that he ‘‘was trying to come up with a number with as few significant figures as I could, considering the precision of what we were dealing with. A minute was too short — an hour was too long’’ [4]. His committee settled on an averaging time of 0.1 hours. That limit evolved in subsequent standards into the 6 minutes found in present exposure limits. The averaging time has been subject to further refinement, including introduction of a complex frequency dependence in IEEE and ICNIRP limits to meet up with the much shorter averaging time specified in exposure limits for infrared radiation (ANSI Z136.1) at the frequency (300 GHz) where the RF and infrared limits meet. The result is the complex set of ‘‘averaging times’’ summarized in Table 1. All this implies a far higher level of precision than the original developers intended.

Despite the increase in complexity of the averaging times (as with other aspects of the RF exposure limits), there have been few published attempts to refine the averaging time in the exposure limits based on thermal analysis of RF heating of tissue. In part this may have been because the averaging times have had little practical effect on assessing compliance of RF sources with safety limits. This may change in the future, for two reasons. First, 5G communications technology, which is on the verge of large-scale introduction, utilizes steerable arrays of millimeter (mm) wave (30-300 GHz) beams, and will result in large temporal variation in exposure at any point in space; proposals [5] for statistical assessment of compliance of transmitters with RF exposure limits are sensitive to the choice of averaging time. Second, high-powered (100 kW) pulsed mm-wave sources are being developed [6] and occupational or nonoccupational exposures to high powered mm-wave pulses cannot be excluded. Currently both IEEE C95.1-2005 and ICNIRP (1998) are undergoing periodic revision, and this is an appropriate time to reconsider the averaging time as it appears in these limits.

We presently consider averaging times at frequencies above the ‘‘transition frequency’’ of 3-10 GHz (depending on the limit), where basic restrictions in both IEEE and ICNIRP limits change from limits on specific absorption rate (SAR) in tissue to incident power density. (These definitions are anticipated to change with prospective revisions in the limits. Both IEEE and ICNIRP limits are proposed to change the definition of basic restrictions above 3-10 GHz to epidermal power density and transmitted power density, respectively.)

We consider the heating characteristics of the surface of the body from exposure to RF energy above 3 GHz, based on the dynamic characteristics of a standard thermal model for tissue, Pennes' bioheat equation (BHTE) [8]. Finally, we consider the resulting implications of this analysis for proper choice of averaging times in the limits. This work builds on recent studies by the present authors [9]–[12].

Using the terminology of systems analysis, the dynamic response of the surface temperature (T_{sur}) is characterized by the step response (rise in temperature from a suddenly imposed exposure). The time derivative of the step response provides the impulse response, which can be convolved with an arbitrary input to find the thermal response of the tissue to time-varying RF exposure. The Laplace transform of the impulse response allows an analysis of the response of the surface temperature to exposures modulated at different frequencies. (In the present discussion, modulation refers to the RF power density, not to the RF field itself).

To avoid misunderstanding, we address thermal hazards only (which are the basis of present RF exposure limits at frequencies above $\approx$1 MHz). In revising the limits, a broader range of scientific data would need to be considered, including reports of possible nonthermal effects.

II. BASELINE MODEL

We consider first a baseline model, using a simplified form of the BHTE, which can be written:

$$k\nabla^2 T - \rho^2 C m_b T + \rho SAR = \rho C \frac{dT}{dt} \quad (1)$$

where T is the temperature rise of the tissue (°C) above the baseline (pre-exposure) temperature at the surface; k is the thermal conductivity of tissue (0.37 W/m °C); SAR is the microwave power deposition rate (W/kg); C is the heat capacity of the tissue (3390 $m^2/s^{2\circ}C$); ρ is the tissue density (1109 kg/m^3), and m_b is the volumetric perfusion rate of blood ($1.8 \cdot 10^{-6}$ $m^3/(kg\ sec)$). Parameter values are from Hasgall *et al.* [13] as used in a commercial finite difference time domain/thermal analysis program and in our previous studies.

We assume a semi-infinite plane of tissue with electrical properties characteristic of skin, exposed to plane wave RF energy incident normally on the surface. This results in an absorbed power density (specific absorption rate or SAR) at the surface:

$$SAR = \frac{I_o(t) T_{tr}}{\rho L} e^{-z/L} \quad (2)$$

where I_o is the incident power density, T_{tr} is the power transmission coefficient into the tissue and L is the energy penetration depth into tissue, which is defined as the distance beneath the surface at which the SAR has fallen to a factor of 1/e below that at the surface. The surface is assumed to have adiabatic boundary conditions (no heat is transferred to the surrounding environment), and the initial surface temperature is assumed to be zero with respect to baseline (pre-exposure) skin temperature.

Exposure is described in terms of a step function u(t)

$$I_o(t) = I_o u(t) \quad (3)$$

where I_o is the intensity of the radiation incident on the surface.

This baseline model has been discussed at length elsewhere [9]–[11] and the initial description (roughly through Eqs. 4a,b) and some previous results have been repeated here to improve the readability of the present paper. The model is highly oversimplified, but nevertheless it provides a reasonable fit to experimental data without further adjustment to model parameters [9]–[11]. Moreover, it admits to simple analytical solutions to compare with numerical solutions to more detailed models. The model works particularly well in the early transient period where the initial thermal response is dominated by heat conduction. By contrast, the steady state temperature is strongly affected by blood perfusion (a highly variable quantity). The homogeneous 1D model does not take into account the comparatively high thermal resistance of subcutaneous fat, which can have a significant effect on the rise on surface temperature after the early transient period [14]. The effect of adiabatic boundary conditions presently assumed, as opposed to more realistic convective boundary conditions (heat exchange with air outside the tissue) is minor for normal room environments due to large temperature gradients just beneath the tissue surface (see the discussion near Eq. 8 in [10]).

Eq. 1 has two intrinsic time scales representing heat transport by blood perfusion and thermal conduction, respectively:

$$\tau_1 = 1/m_b\rho \approx 500 \text{ sec} \quad (4a)$$
$$\tau_2 = L^2/\alpha \quad (4b)$$

where $\alpha = k/\rho C$ is the thermal diffusivity ($\approx 10^{-7}$ m^2/s for soft tissue) and L is a measure of the spatial extent of exposure (for the 1D model presently considered it is the energy penetration depth defined in Eq. 2). The first time constant (τ_1) characterizes heat clearance from the exposed region of tissue by blood perfusion and is the order of 8 min for parameter values assumed here. The second (τ_2) characterizes heat diffusion over a distance comparable to L and varies with frequency of the incident wave. Table 2 summarizes the main characteristics of this model. Below about 3 GHz, $\tau_2 > \tau_1$. In the mm-wave band (30-300 GHz), $\tau_2 \ll \tau_1$ which results in qualitatively quite different transient heating characteristics compared to that at lower frequencies.

A. STEP RESPONSE

The step response for this model in the Laplace domain was obtained using the computer algebra program Maple (Waterloo Maple, Waterloo ON):

$$T_{sur}(s) = \frac{I_0 T_{tr} L}{ks} \frac{(\sqrt{R + s\tau_2} - 1)}{(R - 1 + s\tau_2)\sqrt{R + s\tau_2}} \quad (5a)$$

where

$$R = \frac{\tau_2}{\tau_1} \quad (5b)$$

is the ratio of time constants and s is the Laplace variable. The steady state temperature increase T_{ss} at the surface is

$$T_{ss} = \frac{I_0 T_{tr} L}{k(R + \sqrt{R})} \quad (6)$$

The step response in the time domain $T_{sur}(t)$ is the inverse Laplace transform of Eq. 5a, as shown in Eq. 7 at the bottom of the next page. This result was verified by direct numerical solution of Eq. 1 for several cases using a finite element program PDEase (originally supplied by Macsyma, Inc. but presently sold under the name FlexPDE by PDE Solutions, Spokane Valley, WA). This program has adaptive control of element size and time steps to achieve user-specified error tolerances. Calculations were repeated with progressively smaller error tolerances to ensure that the solution had properly converged and reproduced analytical solutions for test cases.

Eq. 7 (together with most analytical solutions to Eq. 1, e.g. [15]) are cumbersome. We consider analytical results to even more simplified models that provide good approximations to the full solution (Eq. 7) in certain limiting cases.

TABLE 2. Baseline 1D model results, assuming I_o = 100 W/m^2 incident power density.

Frequency, GHz	Power transmission coefficient into skin T_{tr}*	Energy penetration depth L (mm)*	Convection time constant τ_1, sec	Conduction time constant τ_2, sec	R (ratio τ_2/τ_1)	Steady state temperature increase, °C**	Surface heating approximation, steady state temperature increase
1	0.45	19.2	508	3700	7.4	0.23	0.86
3	0.47	9.4	508	904	1.8	0.39	0.91
10	0.49	1.9	508	36	0.072	0.74	0.95
30	0.54	0.43	508	1.8	$3.6 *10^{-3}$	0.98	1.04
100	0.70	0.18	508	0.34	$6.6 *10^{-4}$	1.31	1.34
300	0.84	0.14	508	0.19	$3.9 *10^{-4}$	1.58	1.61

* Calculated from thermal properties of dry skin from [13]
**Calculated from numerical solution of Eq. 1 for an adiabatic half plane of tissue assuming parameters listed below Eq. 1.

B. SURFACE HEATING MODEL

At mm-wave frequencies the energy penetration depth L is small. This suggests a further simplified model that assumes that energy is absorbed at the surface only, which is developed by setting the SAR to zero within the tissue and forcing a thermal gradient of I_oT_{tr}/k directed into the surface. The step response of this model is, in dimensioned form,

$$T_{sur,L=0}(t) = \frac{I_0T_{tr}}{\rho\sqrt{km_bC}} erf\left(\sqrt{\frac{t}{\tau_1}}\right) \tag{8a}$$

$$T_{sur,L=0}(s) = \frac{I_0T_{tr}}{\rho\sqrt{km_bC}}\frac{1}{s\sqrt{s\tau_1+1}} \tag{8b}$$

$$T_{ss,L=0}(s) = \frac{I_0T_{tr}}{\rho\sqrt{km_bC}} \text{as t} \rightarrow \infty \tag{8c}$$

The time domain response (Eq. 8a) is an excellent approximation to Eq. 7 over the entire mm-wave band (30-300 GHz). At lower frequencies the surface heating approximation overpredicts Eq. 7 but the errors down to 10 GHz are modest (Table 2).

The early transient response of the surface heating model (Eq. 8a) can be found by expanding Eq. 8a to first order in t/τ_1. Using the parameter values given with Eq. 1, this becomes [10]

$$T_{sur}(t) = 9.6 * 10^{-4} IoT_{tr}\sqrt{t}°\text{C} \quad (\text{surface heating, t} \ll \tau_1). \tag{8d}$$

C. HEAT CONDUCTION ONLY MODEL

For exposure times $\ll \tau_1$, heat transport by blood flow is negligible compared to heat conduction near the exposed region, and a simple heat conduction model is sufficient (i.e. setting m_b to 0 in Eq. 1). In dimensioned form, the step response of this model assuming adiabatic boundary conditions is:

$$T_{sur}(t) = \frac{I_oT_{tr}L}{k}\left[2\sqrt{\frac{t}{\pi\tau_2}} + \left(e^{\frac{t}{\tau_2}} erfc\left(\sqrt{t/\tau_2}\right) - 1\right)\right] \tag{9a}$$

Expanding Eq. 9a to first order in t/τ_2 yields

$$T_{sur}(t) = \frac{I_oT_{tr}t}{\rho CL} + O\left((\frac{t}{\tau_2})^{3/2}\right) + \ldots \tag{9b}$$

The first term in Eq. 9b is due to heat accumulation in the exposed volume of tissue, neglecting effects of thermal conduction. For mm-waves, this limit is appropriate for short pulses ($\ll$ 1 sec duration). Effects of blood perfusion become apparent in the BHTE model only over much longer times (minutes).

D. IMPULSE RESPONSE

The impulse response is the time derivative of the step response (Eq. 5a or 7), which is most conveniently obtained via Laplace transform:

$$L^{-1}(sT_{sur}(s))/T_{ss} = \frac{1}{\tau_1}\left(1+\frac{1}{\sqrt{R}}\right)e^{\left(\frac{1}{\tau_2}-\frac{1}{\tau_1}\right)t} erfc\left[\sqrt{\frac{t}{\tau_2}}\right] \tag{10a}$$

where $L^{-1}(\ldots)$ is the inverse Laplace transform. Expansion about t=0 yields

$$L^{-1}(sT_{sur}(s))/T_{ss} \approx \frac{1+\sqrt{1/R}}{\tau_1}\left(1-1.13\sqrt{\frac{t}{\tau_2}}\right) \tag{10b}$$

for the increase in surface temperature normalized by the steady state temperature increase T_{ss}. In the limit as t→0 this

$$T_{sur}(t)/T_{ss} = 1 + \frac{erfc\left(\sqrt{\frac{t}{\tau_2}}\right)e^{-t/\tau_1+t/\tau_2}(\tau_2+\sqrt{\tau_1\tau_2}) - erfc\left(\sqrt{\frac{t}{\tau_1}}\right)(\sqrt{\tau_1\tau_2})+\tau_1)}{(\tau_1+\tau_2)} \tag{7}$$

becomes, in dimensioned form

$$L^{-1}(sT_{sur}(s)) \rightarrow \frac{I_o T_{tr}}{\rho CL} \quad \text{as t} \rightarrow 0. \tag{10c}$$

as expected from Eq. 9b. The impulse response of the surface heating model calculated from Eq. 8a diverges as $t^{-1/2}$ in the limit t→0.

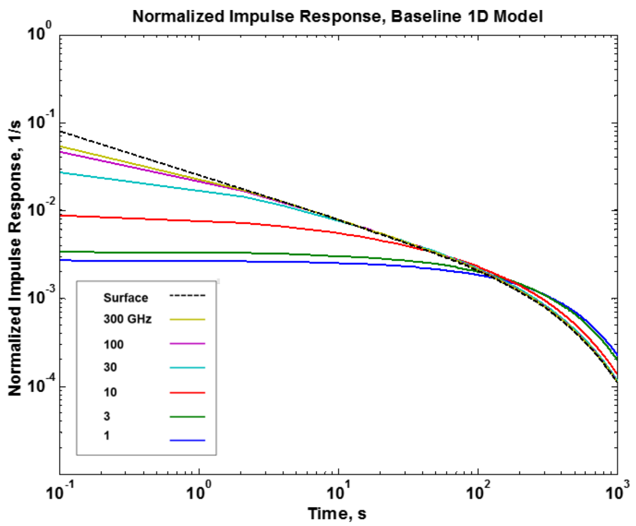

FIGURE 1. **Impulse response of surface temperature increase for the baseline 1D model, normalized by steady state temperature rise at the surface, at several frequencies (Eq. 10a and Eq. 6). Also shown is the normalized impulse response for the surface heating model (-----), which is the time derivative of *erf* ($\sqrt{t/\tau_1}$) (cf. Eq. 8a,c).**

Fig. 1 shows the impulse response for the 1D model (Eq. 10a) for incident energy at various frequencies. At mm-wave frequencies, the impulse response has a strong spike at short times, followed by a long tail that persists for hundreds of s. The integral of the normalized impulse response (Eq. 10a) (i.e. the normalized step response) over all time has a value of 1. For the parameter values presently assumed, fifty percent of this integral occurs within about 100-300 s of the impulse, but a significant tail exists for considerably longer times due to the slow removal of heat by blood perfusion (Table 3).

For a time-varying exposure, the increase in surface temperature is given by the convolution of 10a with the input power density, which provides a definition of time-averaging of exposure. The sharp peak in the impulse response for short times at mm-wave frequencies means that the convolution will strongly weigh the short-term response at mm-wave frequencies but will include significant contributions for much longer times as well (Table 3). Below the mm-wave band, the impulse response lacks the peak at short times and the convolution will more closely approximate time averaging using a rectangular window of several minutes' duration.

TABLE 3. **Time for 90% of integrated impulse response.**

F, GHz	Time for 50% integrated impulse response, s	Time for 90% integrated impulse response, s
1	294	1032
3	258	952
10	172	779
30	133	712
100	123	699
300	121	697
Surface heating	116	689

III. TRANSIENT HEATING BY RF PULSES

The above simple models yield simple expressions for the transient increase in temperature produced by a brief pulse of duration $\Delta\tau$. Depending on the pulse duration relative to τ_2:

$$\Delta T = \frac{I_o T_{tr}}{\rho CL}\Delta\tau, \quad \Delta\tau \ll \tau_2 \ll \tau_1 \quad \text{(from Eq. 9b)} \tag{11a}$$

$$= 9.6 \cdot 10^{-4} I o T_{tr}\sqrt{\Delta\tau}, \quad L \rightarrow 0,\ \tau_2 < \Delta\tau \ll \tau_1 \quad \text{(from Eq. 8d)} \tag{11b}$$

Thus, the transient temperature increase after each pulse will be proportional to either the fluence of the pulse ($I_o\Delta\tau$) (Eq. 11a) or to the fluence divided by $\sqrt{\Delta t}$ (Eq. 11b).

We consider three cases:

Pulse Train: We consider the thermal response to a train of 1 s pulses with a repetition rate of 0.1 Hz and power density of 1000 W/m^2 (pulse fluence 1000 J/m^2) and time-averaged incident power density of 100 W/m^2. This is twice the time-averaged FCC occupational exposure limits between 1.5-100 GHz, and twice the basic restrictions for occupational exposures between 2-300 GHz in the proposed (Aug. 2018) revision of ICNIRP guidelines.[1] This waveform was chosen for purposes of illustration, and is not characteristic of exposures from commonly used technologies.

Fig. 2 shows the numerically calculated increase in surface temperature from this pulse train with different carrier frequencies. (Responses at 300 GHz are indistinguishable from those at 100 GHz and are not shown). Fig. 2 also shows the corresponding temperature increases from exposure to continuous wave (CW) exposure radiation at the same time-averaged power level, 100 W/m^2. The transient increases after each pulse agree well with the theory (Table 4). In addition, the secular (slow) increase from CW exposure is consistent with the DC component of the modulation waveforms. At 100 GHz and above, $\tau_2 < 1$ s. For pulses shorter than 1 s, the transient temperature increase after each pulse will vary as the inverse of the pulsewidth up to limit given in Eq. 11a.

"Big Bang Pulse": We consider the response to a single pulse of duration $\Delta\tau$ and fluence ($I_o\tau_{avg}$), which is the

[1] ICNIRP public consultation document, https://www.icnirp.org/en/activities/public-consultation/index.html, accessed 24 August 2018

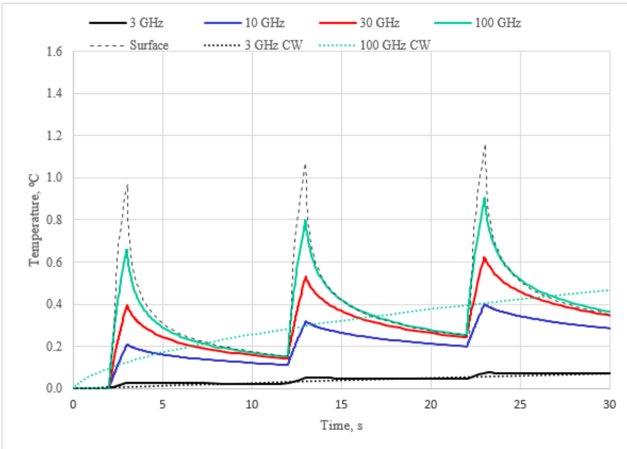

FIGURE 2. **Skin surface temperature increase in 1D baseline model to pulse train at varying carrier frequencies in GHz and for the surface heating model for comparison. Pulses are 1 s duration, repeated at 1/10 Hz, peak pulse intensity 1000 W/m^2. Also shown (dotted lines) are the increases in surface temperature from exposure to continuous-wave radiation at the same time-averaged power density at 3 and 100 GHz. The energy transmission coefficient was assumed 1 at all frequencies to facilitate comparisons of responses.**

TABLE 4. **Transient Responses to Pulse Train in Fig. 2: Comparison of analytical and numerical results.**

f, GHz	Transient temperature increase after each pulse, numerical simulation °C	Transient temperature increases after each pulse, from (Eq. 7). °C	Steady state temperature increase (°C) from CW exposure at same time-averaged power density
3	0.028	0.028	0.8
10	0.12	0.12	1.5
30	0.39	0.39	1.8
100	0.63	0.61	1.9
300	0.66	0.67	1.9
Surface heating	0.96	0.96	1.9

maximum fluence pulse permitted under the limit I_o subject to averaging time τ_{avg} (here assumed to be 6 min). This is the most extreme exposure scenario that would be permitted under the constraints of the limits on time-averaged power density and averaging time.

The thermal transients produced by the ''big bang'' pulses (Fig. 3) at mm-wave frequencies are as much as 20 times higher than the temperature increases from CW exposure in the steady state. Such ''big bang'' exposures represent extreme cases that would hardy ever or never be encountered in the real world but are considered as a limiting case. One exception is a military nonlethal weapons system [6].

Communications (GSM) Waveform: To illustrate the implications of the above for more realistic waveforms, we consider the transient temperature fluctuations produced by a simulated GSM waveform with a single occupied timeslot (0.57 ms pulse width, 217 Hz repetition rate, duty cycle of 0.125). The time averaged power level is 100 W/m^2 (above

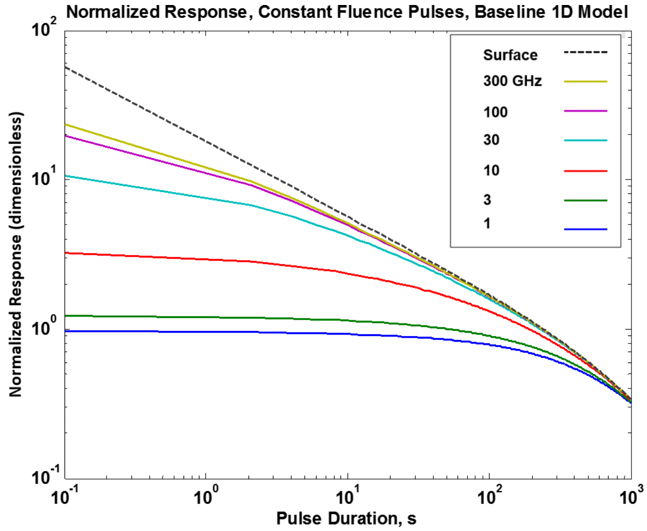

FIGURE 3. **Peak transient increase in surface temperature in 1D baseline model produced by a single ''big bang'' pulse of constant fluence ($I_o\tau_{avg}$) vs. pulse duration. Results are normalized by the steady-state temperature increase for CW exposures at power density I_o Averaging time τ_{avg} is 6 min.**

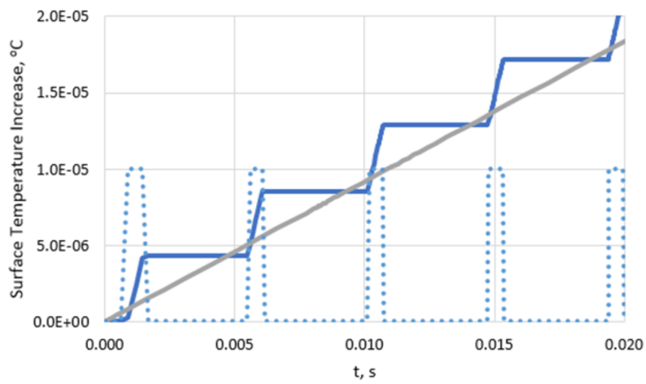

FIGURE 4. **Surface temperature increase from pulse train similar to that produced by GSM access technology with one timeslot occupied. Pulse width 0.57 ms, repeated at 217 Hz, pulse power density 800 W/m^2, fluence of each pulse 0.45 J/m^2. Time averaged power density is 100 W/m^2 at 1.9 GHz; energy transmission coefficient into tissue T_{tr} = 0.46. Also shown (solid line) is the increase in surface temperature from CW radiation at the same frequency and time-averaged power density. Pulses shown by dotted line. Steady state temperature increase from CW exposure at this average power density is 0.3 C.**

regulatory limits). The peak power density during a pulse is 800 W/m^2 and the pulse fluence is 0.46 J/m^2. The carrier frequency is 1.9 GHz and the power transmission coefficient into the skin is 0.47. The resulting temperature transients are very tiny (4 microdegrees C) (Fig. 4). The magnitude of these transients agrees well with Eq. 11a.

The small magnitude of the thermal transients in Fig. 4 is a consequence of a carrier frequency (1.9 GHz) that is far below the mm-wave band and of the small fluence of the pulses compared to a ''big bang''. While same waveform at mm-wave frequencies would produce larger thermal transients, it seems unlikely that any communications waveform would have extreme modulation characteristics sufficient to produce thermal transients that even approach the steady-state increase in temperature.

IV. FREQUENCY RESPONSE

It is useful to consider the response of the BHTE in the frequency domain (referring to the frequency content of the SAR, not of the carrier wave). Exposure to a periodic waveform can be decomposed into a secular (DC) component representing time-averaged exposure together with components at varying frequencies. Consequently, it is useful to consider the thermal response of the BHTE in the frequency domain.

For a time-varying input $I_o(s)$, a transfer function between the surface temperature and exposure $T_{sur}(s)/I_o(s)T_{ss}$ can be written

$$\frac{T_{sur}(s)}{I_0(s)T_{ss}} = \frac{(R+\sqrt{R})(\sqrt{R}\sqrt{1+s\tau_1}-1)}{\sqrt{R}\sqrt{1+s\tau_1}(R+s\tau_1 R-1)} \tag{12a}$$

$$\approx \frac{1}{1+s\tau_1}, \quad R \gg 1 \tag{12b}$$

$$\approx \frac{1}{\sqrt{1+s\tau_1}}, \quad R \ll 1 \tag{12c}$$

The transition between these limiting cases occurs at approximately R=1, corresponding to about 4 GHz.

The steady state response to sinusoidal input $I_o\sin(\omega\, t)$ is obtained by substituting $s=j\omega$ in Eq. 12a, where ω is the radian frequency and $j = \sqrt{-1}$. Eqs. 12a-c represent an extreme lowpass filter with cutoff frequency of $1/(2\,\pi\tau_1)$ ($\approx$ 0.3 mHz for the blood flow parameter presently assumed).

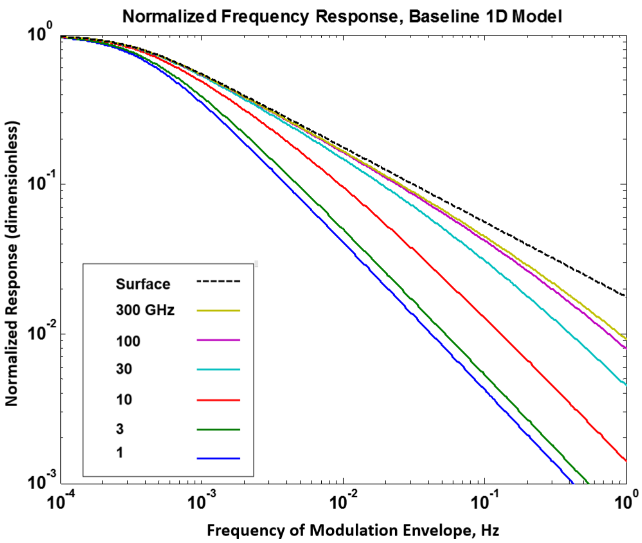

FIGURE 5. Frequency response of baseline 1D model, normalized by steady state temperature rise at the surface, at several frequencies. The very low cutoff frequency, ≈ 0.3 mHz, is a consequence of the relatively slow removal of heat by blood perfusion, while the high frequency response is chiefly attributable to heat conduction through the layer of tissue in which the energy is absorbed. Also shown is the frequency response for the surface heating model (Eq. 8b).

Figure 5 shows the normalized frequency response of the 1D baseline model (Matlab, Mathworks, Natick MA). The extreme lowpass filtering properties of the bioheat equation are evident. The higher gain of this transfer function at mm-wave frequencies correlates with the larger thermal transients from pulsed waveforms in the mm-wave band (Fig. 2).

V. MORE REALISTIC MODELS

For comparison with the simple 1D baseline model we consider two more realistic models based on Morimoto *et al.* [12]. That study determined RF exposure in multilayer planes of tissue and also detailed image-based models using the finite difference time domain (FDTD) method followed by numerical solution to the BHTE, with convective boundary conditions appropriate for a human in normal room environment. The planar model in [12] was recalculated for the present study assuming a semi-infinite layered plane exposed to plane wave radiation, using blood flow parameter given above in Eq. 1. The step and impulse responses for the multilayer planar model are in Fig. 6.

In addition, we considered the step response for exposure to the head of an image-based Japanese male model known as "Taro," using data originally shown in Fig. 6 in [12]. The original data from [12] were upsampled by a factor of 3 using the Matlab command "interp" to allow display of the frequency response up to 0.1 Hz without aliasing artifacts. The exposure source consisted of a resonant dipole located 1.5 cm from the head and opposite the ear as shown in Fig. 2 of [12], and the temperature increases were the peak increases anywhere in the head (which generally occurred in the pinna or in superficial tissues of the head near the pinna, but varying somewhat in location with frequency). The impulse and frequency responses are shown in Fig. 7, and the step responses of the models are compared in Table 5 in comparison with the surface heating model.

The responses of all of these models are remarkably similar despite differences in boundary conditions, geometry, and differences in the models. The steady state temperature increase in the baseline model is slightly higher than in the multilayer planar model, which may be due to the different boundary conditions (adiabatic in the 1D model vs. convective for the other two). The response times of the multilayer plane model are roughly 20% longer than those of the 1D model. In addition, the head model shows a somewhat faster thermal response than the other models, which may result from the lower thermal inertia of the pinna.

The similarities in the thermal responses across all of the models considered here is chiefly due to the fact that the thermal response at short times reflects heat conduction over short distances because of the frequency range presently considered. The governing parameter, the thermal conductivity, is generally similar in different high-water content tissues [13]. By contrast, thermal washout from blood perfusion is far more variable, but occurs over relatively much longer time scales. Numerous calculations reported in [12] and elsewhere show similar step responses in surface temperature and we do not expect that results with different anatomical models will vary sufficiently to affect the general conclusions of this present study. However, this present study considers only exposure to plane waves or radiation from a dipole antenna located 1.5 cm from the body Exposures from a very localized source with small beam width will introduce

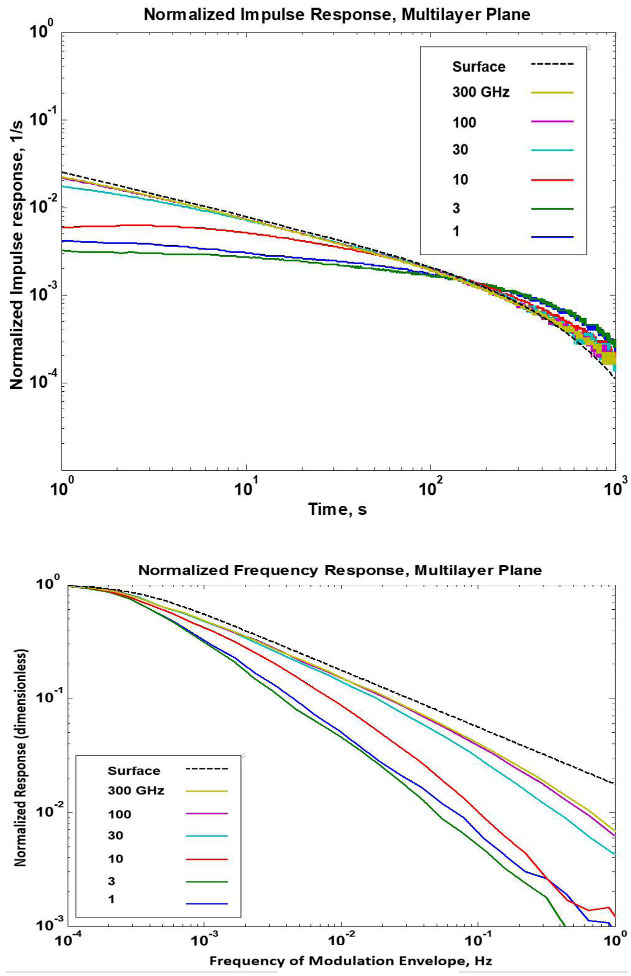

FIGURE 6. **a,b. Impulse and frequency response of multilayer plane, compared to respective responses for surface heating model. Results are for the multilayer model described in [12]. Results are normalized by the steady state temperature increases (Eq. 12). Exposure was to plane wave radiation at indicated frequencies, the responses of the surface heating model shown for comparison.**

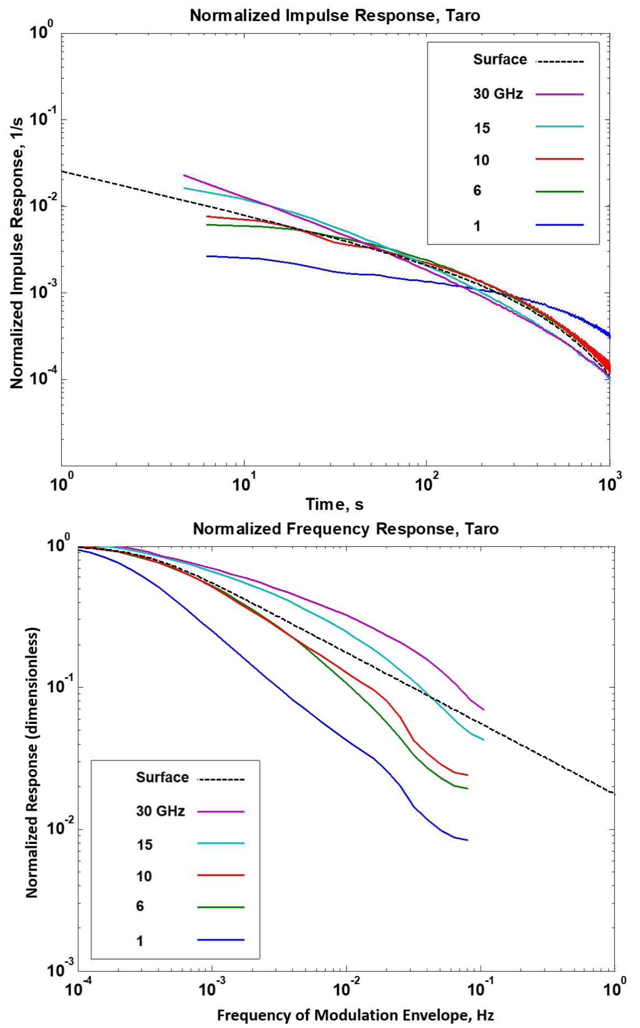

FIGURE 7. **a,b. Impulse and frequency response of RF exposure to the head of an anatomically detailed human model (Taro). Results are from [12], upsampled to allow display of frequency response without aliasing. The exposure source was a resonant dipole located 1.5 cm from the head and opposite the ear as shown in Fig. 2 of [12]. Responses of the surface heating model are shown for comparison.**

other timescales into the problem due to thermal conduction away from the source. Heat transfer near major blood vessels will introduce still other short response times.

VI. COMMENTS ON EXPOSURE LIMITS

The above analysis shows that the thermal response of tissue is characterized by two timescales, one much shorter than the other at mm-wave frequencies. Very short mm-wave pulses with high fluence can produce significant temperature transients at the tissue surface. These exposures are seldom if ever encountered in the real world but may be produced by specialized technologies including some military weapons systems. At lower frequencies, and for mm-waves with more modest crest factors, the slower response will dominate.

It appears that present exposure limits are generally protective against excessive skin heating from mm-waves, although special cases might be considered where thermal pain sensations might be elicited under extreme exposure conditions. Present FCC limits are 10 W/m^2 for the general public at frequencies above 1.5 GHz (averaging time 30 min) and 50 W/m^2 for occupational groups (6 min averaging time). In both cases, the maximum fluence in a single ''big bang'' pulse that would compliant with FCC limits (i.e. the limit for CW exposures times the averaging time) is 18,000 J/m^2. For comparison, Walters *et al.* [16] determined a threshold fluence of 38,000 J/m^2 for 3 second pulses of 94 GHz radiation to elicit cutaneous thermal pain. Given the inverse square root dependence of temperature increase on fluence (Eq. 11b) it appears that the FCC limits might not protect against thermal pain produced by very brief (< 1 s) pulses of maximally allowable fluence. Such exposures are seldom or never encountered in the real world.

Present editions of both the ICNIRP and IEEE guideline/standards limit the fluence of short pulses indirectly through choice of averaging time. IEEE C95.1-2005 limits in the upper tier are 100 W/m^2 above 3 GHz, with the averaging

TABLE 5. Comparison of step response of the three models.

Frequency, GHz	Steady state temperature increase, °C**	Step response: time to reach 90% of steady state temperature increase, sec	Step response: time to reach 90% of steady state temperature increase, sec Baseline model (Eq. 1)
Image-based human head model (Taro) (1 W resonant dipole)			
1	0.81	1560	
6	1.40	854	
10	1.69	854	
15	1.73	624	
30	1.92	648	
Multilayer plane model (I_o = 100 W/m^2); T_{tr} varies with frequency			
1	0.25	1143	
3	0.29	1109	925
10	0.54	1009	775
30	0.87	848	800
100	1.21	865	650
300	1.47	876	650

** From Fig. 6 of [12]

time ranging downwards from 6 min (3 GHz) to 10 s at 300 GHz. The maximum fluence of a pulse at 100 GHz consistent with the averaging time of 16.9 s at that frequency in the IEEE standard would be 1690 J/m^2. The maximum transient increase in surface temperature from a short pulse with that fluence would be about 2.5 °C (from Eq. 11a). ICNIRP (1998) imposes similar fluence limits on such pulses.

Presently both IEEE and ICNIRP limits are in process of revision. We offer general comments related to the choice of averaging time, particularly as related to limits for millimeter waves. Several approaches are available that vary in efficiency, i.e. in preventing excessive temperature increase from high-fluence mm-wave pulses without imposing undue restrictions on less extreme and thermally innocuous exposures from commonplace technologies.

The simplest approach is to simply reduce the averaging time to limit, in effect, the maximum allowable fluence of a pulse. One strategy (which was suggested by one of us in [17]) would be to choose an averaging time such that the temperature rise produced by a single maximum ''big bang'' pulse (Eq. 11a) will be the same as that produced by continuous exposure at the limit at the same frequency. This approach will be protective against thermal pain or damage from very brief high-fluence pulses. However, it is inefficient in that the resulting short averaging time would also exclude time-varying exposures from commonplace technologies that have negligible thermal impact.

More efficient approaches are possible, with varying levels of refinement. These might include:

(a) *Improved Averaging Process:* The ''averaging time'' specified in IEEE and ICNIRP limits implies calculating a moving average of the exposure over time, in effect using a rectangular window. A more correct approach would be to calculate a weighted moving average using a window function that approximates the impulse function of the BHTE at the appropriate carrier frequency (Eq. 10a). An intermediate approach would be to express the impulse response as a superposition of short and long-time components, where the thermal response to the short-time component would be negligible except for extreme waveforms with high fluence pulses. These would be straightforward signal processing operations but may be impractical for several reasons. Moreover, for nearly all real-world exposures, that level of refinement would be difficult to justify.

(b) *Establishing a Fluence Limit for RF Pulses:* This is a practical approach for pulsed waveforms, which would be used in addition to the present 6-minute averaging time for average power density. However, a fluence limit that would be adequately protective for very short mm-wave pulses would be excessively conservative for longer pulses, and highly overconservative below the mm-wave band.

(c) *Setting a Limit on Fluence That Depends on Frequency and Pulsewidth Based on the Full Theory Described Here, e.g. Eq. 7:* This refinement of approach (b) could provide a more consistent level of protection against excessive temperature increase, but the resulting limits may be impractically complex.

(d) *Setting a Fluence Limit for mm-Wave Pulses Only, Based on an Approximate Thermal Model:* In the surface heating model, the transient increase in surface temperature scales as the square root of the pulse duration (Eq. 8d). This implies that the fluence in a single pulse of duration τ should be limited to about $10^3\tau^{1/2}$J/m^2 (where τ is in s) to limit transient temperature increases to about 1 °C. This would be a relatively simple approach that, at mm-wave frequencies, relies on a model that is a good approximation to a decidedly more complex thermal response of tissue. In any case, the standards setting committee would have to be clear what level of thermal transients would be tolerable.

The heat transfer theory based on the BHTE (Eq. 1) has experimental support, particularly as related to thermal response to brief RF pulses where heat conduction effects dominate. In particular, limited data from human subjects exposed to mm-wave pulses at 96 GHz agree well with the theory presented above with no adjustable parameters [16]. However, additional experimental evidence is needed over a wider range of exposure conditions and frequencies to improve the experimental basis for setting exposure limits.

VII. CONCLUSION

Heretofore, the ''averaging time'' has not been a large issue in designing exposure limits. In previous limits it has been set largely on an *ad hoc* basis (or on back-of-the-envelope calculations as described by Ely [4]) with little attempt to optimize the choice. For most real-world applications of the limits, the question is how long an individual can be allowed to remain in a field at a given exposure level, and an approximate calculation of averaging time is probably adequate considering the many other uncertainties that are involved. However a more refined approach is needed due to the widespread adoption of mm-wave technology including emergence of 5G communications systems and the development of high powered pulsed mm-wave sources for military and industrial applications. These will result in highly variable exposures to individuals in both occupational and nonoccupational settings, possibly at high peak levels in some cases. A more extensive and experimentally supported analysis of the thermal consequences of such exposures is needed, both to design adequately protective exposure limits as well as to avoid excessive conservatism in protection against thermal hazards.

REFERENCES

[1] *Evaluating Compliance with FCC Guidelines for Human Exposure to Radiofrequency Electromagnetic Fields*, FCC Bulletin OET 65, Washington, DC, USA, 1997.

[2] *IEEE Standard for Safety Levels with Respect to Human Exposure to Radio Frequency Electromagnetic Fields, 3 kHz to 300 GHz*, IEEE Standard C95.1-2005, 2010.

[3] A. Ahlbom *et al.*, ''Guidelines for limiting exposure to time-varying electric, magnetic, and electromagnetic fields (up to 300 GHz),'' *Health Phys.*, vol. 74, no. 4, pp. 494–521, 1998.

[4] K. R. Foster, A. Lozano-Nieto, P. J. Riu, and T. S. Ely, ''Heating of tissues by microwaves: A model analysis,'' *Bioelectromagnetics*, vol. 19, no. 7, pp. 420–428, 1998.

[5] B. Thors, A. Furuskär, D. Colombi, and C. Törnevik, ''Time-averaged realistic maximum power levels for the assessment of radio frequency exposure for 5G radio base stations using massive MIMO,'' *IEEE Access*, vol. 5, pp. 19711–19719, 2017.

[6] N. Kumar, U. Singh, A. Kumar, and A. K. Sinha, ''Design of 95 GHz, 100 kW Gyrotron for active denial system application,'' *Vacuum*, vol. 99, pp. 99–106, Jan. 2014.

[7] C.-K. Chou *et al.*, ''Revision of IEEE standards C95.1-2005 and C95.6-2002,'' in *Proc. BioEM Piran*, Portoroz, Slovenia, Jun. 2018, pp. 326–331.

[8] H. H. Pennes, ''Analysis of tissue and arterial blood temperatures in the resting human forearm,'' *J. Appl. Physiol.*, vol. 1, no. 2, pp. 93–122, 1948.

[9] K. R. Foster, M. C. Ziskin, and Q. Balzano, ''Thermal response of human skin to microwave energy: a critical review,'' *Health Phys.*, vol. 111, no. 6, pp. 528–541, 2016.

[10] K. R. Foster, M. C. Ziskin, and Q. Balzano, ''Thermal modeling for the next generation of radiofrequency exposure limits: commentary,'' *Health Phys.*, vol. 113, no. 1, pp. 41–53, 2017.

[11] K. R. Foster, M. C. Ziskin, Q. Balzano, and G. Bit-Babik, ''Modeling tissue heating from exposure to radiofrequency energy and relevance of tissue heating to exposure limits: Heating factor,'' *Health Phys.*, vol. 115, no. 2, pp. 295–307, 2018.

[12] R. Morimoto, A. Hirata, I. Laakso, M. C. Ziskin, and K. R. Foster, ''Time constants for temperature elevation in human models exposed to dipole antennas and beams in the frequency range from 1 to 30 GHz,'' *Phys. Med. Biol.*, vol. 62, no. 5, pp. 1676–1699, 2017.

[13] P. A. Hasgall *et al.* (Sep. 2015). *IT'IS Database for Thermal and Electromagnetic Parameters of Biological Tissues, Version 3.0*. [Online]. Available: https://itis.swiss/virtual-population/tissue-properties/downloads/database-v4-0/

[14] M. C. Ziskin, S. I. Alekseev, K. R. Foster, and Q. Balzano, ''Tissue models for RF exposure evaluation at frequencies above 6 GHz,'' *Bioelectromagnetics*, vol. 39, no. 3, pp. 173–189, Apr. 2018.

[15] K. R. Foster, H. N. Kritikos, and H. P. Schwan, ''Effect of surface cooling and blood flow on the microwave heating of tissue,'' *IEEE Trans. Biomed. Eng.*, vol. BME-25, no. 3, pp. 313–316, May 1978.

[16] T. J. Walters, D. W. Blick, L. R. Johnson, E. R. Adair, and K. R. Foster, ''Heating and pain sensation produced in human skin by millimeter waves: Comparison to a simple thermal model,'' *Health Phys.*, vol. 78, no. 3, pp. 259–267, 2000.

[17] K. R. Foster, H. Zhang, and J. M. Osepchuk, ''Thermal response of tissues to millimeter waves: implications for setting exposure guidelines,'' *Health Phys.*, vol. 99, no. 6, pp. 806–810, 2010.

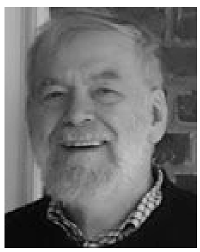

KENNETH R. FOSTER (M'77–SM'81–F'88–LF'13) received the Ph.D. degree in physics from Indiana University Bloomington, Bloomington, IN, USA, in 1971. He was with the U.S. Navy, Naval Medical Research Institute, Bethesda, MD, USA, from 1971 to 1976. Since 1976, he has been with the Department of Bioengineering, University of Pennsylvania, Philadelphia, PA, USA, where he is currently the Professor Emeritus. He has been involved in studies on the interaction of nonionizing radiation and biological systems, including mechanisms of interaction and biomedical applications of radio frequency and microwave energy. He has written widely about scientific issues related to possible health effects of electromagnetic fields. He has authored approximately 160 technical papers in peer-reviewed journals, numerous other articles, and two books related to technological risk and the law. He is a longtime member of TC 95 of the IEEE International Committee on Electro-magnetic Safety and a member of the Physical Agents Committee of the American Conference of Industrial Hygienists, among many other professional activities. In 2016, he received the d'Arsonval Award from the Bioelectromagnetics Society for contributions to the field of bioelectromagnetics. He has been active for many years on the IEEE EMBS Committee of Man and Radiation, the IEEE Society on Social Implications of Technology, and the IEEE Engineering in Medicine and Biology Society. He is a Co-Editor-in-Chief of BioMedical Engineering Online.

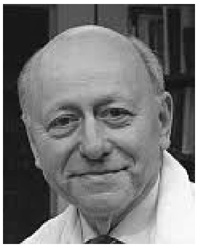

MARVIN C. ZISKIN (M'69–SM'74–LSM'01–F'03–LF'03) received the A.B. and M.D. degrees from the Temple University School of Medicine, Philadelphia, PA, USA, and the M.S.Bm.E. degree in bioengineering from Drexel University. From 1965 to 1966, he was a Research Associate in diagnostic ultrasound at the Hahnemann Medical College. Following a two year tour duty at the U.S. Air Force Aerospace Medical Research Laboratories, he returned to Temple University in 1968, and for the past 23 years he has served as the Director of its Center for Biomedical Physics. From 1982 to 1984, he was the President of the American Institute of Ultrasound in Medicine, and from 2003 to 2006 he was the President of the World Federation of Ultrasound in Medicine and Biology. He is currently a Professor Emeritus of radiology and medical physics at the Temple University School of Medicine. His interest in ultrasound, image processing, and non-ionizing electromagnetic radiation has resulted in seven books and over 275 scientific publications. His research interests include many areas within biomedical engineering with a special interest in ultrasound, millimeter waves, and other non-ionizing radiation. He was the Chairman of the IEEE Committee on Radiation and Man. He is currently the Co-Chair of the IEEE International Committee for Electromagnetic Safety Subcommittee SC4, which establishes safety standards for RF radiation. He has been on the Board of Director of the Bioelectromagnetics Society and the National Council for Radiation Protection and Measurements. He received the 2011 D'Arsonval Award of the Bioelectromagnetics Society. He has served on the editorial boards of the *Journal of Clinical Ultrasound*, *Clinical Diagnostic Ultrasound*, *Ultrasound in Medicine and Biology*, the *Journal of Ultrasound in Medicine*, and *Bioelectromagnetics*. He has been active in a number of professional societies.

QUIRINO BALZANO (S'63–M'72–SM'83–F'02–LF'05) received the Ph.D. degree in electronics engineering from the University of Rome, La Sapienza, Rome, Italy, in 1965. In 1966, he was at FIAT, SpA, Turin, Italy. From 1967 to 1974, he was with the Missile Systems Division, Raytheon Co., Bedford, MA, USA. He was involved in the research, design and development of planar and conformal phased arrays for the Patriot and other missile systems. In 1974, he joined Motorola, Inc., Portable Products Division, Plantation, FL, USA, where he achieved the position of Corporate Vice President and the Director of the Portable Products Research Laboratories. His group was essential in the development of the cell phone technology. He retired from Motorola in 2001. Since 2002, he has been at the ECE Department, University of Maryland at College Park, College Park, MD, USA, where he is currently a Senior Staff Researcher. He teaches courses on antennas at American, European, and Asian universities. His main interest is in antennas, the biological effects of human exposure to RF electromagnetic energy and electromagnetic interference with medical devices. He has written more than 50 papers on antennas, RF dosimetry near electromagnetic sources, and the biological effects of RF energy. He holds 31 patents in antenna and IC technology. He has authored or co-authored more than 120 papers and publications. He received the IEEE Vehicular Technology Society Best Paper of the year Award in 1978 and 1982, respectively, and a certificate of merit from the Radiological Society of North America in 1981 for the treatment of tumors with RF energy. He is the past (2005) Chair of Commission A (Measurements) of the International Union of Radio Science.

AKIMASA HIRATA (S'98–M'01–SM'10–F'17) received the B.E., M.E., and Ph.D. degrees in communications engineering from Osaka University, Suita, Japan, in 1996, 1998, and 2000, respectively. From 1999 to 2001, he was a Research Fellow of the Japan Society for the Promotion of Science, and also a Visiting Research Scientist at the University of Victoria, Victoria, BC, Canada, in 2000. In 2001, he joined the Department of Communications Engineering, Osaka University, as an Assistant Professor. In 2004, he moved to the Nagoya Institute of Technology as an Associate Professor, where he is currently a Professor (Director). His research interests include electromagnetics and thermodynamics in biological tissue, waveguide analysis, EMC and EMI, and computational techniques in electromagnetics. He is a fellow of the Institute of Physics, and a member of IEICE, IEE Japan, and the Bioelectromagnetics Society. He received several awards, including Prizes for Science and Technology (Research Category 2011, Public Understanding Promotion Category 2014) by the Commendation for Science and Technology by the Minister of Education, Culture, Sports, Science, and Technology, Japan, and the IEEE EMC-S Technical Achievement Award in 2015, and the Japan Academy Medal in 2018. From 2006 to 2012, he was an Associate Editor of the IEEE Transactions on Biomedical Engineering. He is an Editorial Board Member of physics in medicine and biology, a member of the main commission and a Chair of the Project Group of the International Commission on Non-Ionizing Radiation Protection, and the Subcommittee Chair of the IEEE International Committee on Electromagnetic Safety, and an expert of World Health Organization.